

COMPUTER PROGRAM FOR SIMPLIFIED EVALUATION OF GAS RADIATION IN TURBINE ENGINE ENCLOSURES

T. Rodríguez, L.M. Rodríguez
(ITP Accessories & Systems Group)

Abstract

Gas radiation is an important heat input to the walls exposed to an afterburning process in a turbojet engine, specially if they are submitted to film cooling or if gas convection is not important on their surface. Hence, it is necessary to take into account this kind of heat in the thermal analysis of the engine components implied.

Some commercial software packages for thermal analysis are able to evaluate radiation heat transfer from solid surfaces. However, there is not a commercial software available which is capable of calculating radiation heat transfer from a gas volume, and less so when a luminous gas is involved in the process.

On the other hand, the study of gas radiation is a complex and expensive subject because of the amount of factors on which the gas radiation properties depend (shape of gas volume, wavelength, emission of soot particles formed because of incomplete combustion, directional properties of emission and absorption...).

The aim of this work is to present a computer program that uses a simplified approach to evaluate the radiation heat fluxes incident on the walls exposed to a hot luminous gas, and its application to the thermal analysis of a military turbojet thrust augmentor.

List of symbols

A: area (m^2)
f: fuel-air ratio
F: view factor
G: irradiation (W/m^2)
J: radiosity (W/m^2)

L: luminosity factor
N: number of cells dividing enclosure surface
P: pressure (KPa)
Q: heat (W)
r: ray length (m)
T: temperature (K)
 α : absorptivity
 ϵ : emissivity
 ϑ : angle
 ρ : reflectivity
 σ : Stefan-Boltzman constant ($5.67E-8 Wm^{-2}K^{-4}$)
 τ : transmittance

subscripts:

g: gas
w: wall

1 Methodology

Gas radiation is a complex subject [4]. Firstly, it is characterized for its discontinuity throughout the wavelength spectrum. There are only a few wavelengths in which radiation is emitted by a gas (those corresponding to the vibration frequency of the atoms within the molecule). Number, width, and emissive power of the different band spectra depend on pressure, temperature, gas composition and thickness of the gas volume.

Another important factor that affects thermal radiation in gases generated by gas turbine fuels is the presence of solid particles. In this case, it has to be added to the "nonluminous" radiation produced by CO_2 , H_2O steam, and others hot heteropolar gases, the "luminous" radiation that is caused by the soot. Thus, in addition to the previous, emission becomes also dependent on particle radiation

properties and particle distribution and concentration.

Luminous radiation intensity raises with pressure because of the increase in size and concentration of the suspended dust. In low-pressure systems (such as an afterburner), it can be introduced a correction in the non-luminous gas emissivity for evaluating the luminous radiation: the luminosity factor (L). This factor has high dependency on the combustible molecule carbon-mass/hydrogen-mass ratio (C/H) [1].

In this study L is determined as:

$$L = 3(C/H - 5.2)^{0.75} \quad (1)$$

The luminosity factor may vary along the flow path, as gradual burnout of soot particles occurs. However, in this study L as well as the overall gas composition are considered constant

Gas emissivity can be evaluated by the program using three correlations valid for pressures beneath 500 KPa [1], although it is also possible in the program to consider a constant value.

When luminous gas, the formula used is the following:

$$\varepsilon_g = 1 - \exp\left[-290P_g L(f \cdot r)^{0.5} T_g^{-1.5}\right] \quad (2)$$

Nonluminous gas emissivity is obtained by removing L from the previous equation, and the third correlation, that may want to be used for low emissivity gases is:

$$\varepsilon_g = 290 \cdot P_g \cdot (f \cdot r)^{0.5} \cdot T_g^{-1.5} \quad (3)$$

On the other hand, the gas inside is considered nonreflecting and nontransparent. Thus, it absorbs part of the radiation coming from the walls, allowing the rest to be transmitted. The gas absorptivity formula used depends on that used for the emissivity, because it is obtained by modifying equations (2) and (3): in (2), L is removed (luminosity only affects emission), then gas temperature is substituted by wall temperature, the beam length by $r \cdot T_w/T_g$, and

finally the whole expression is multiplied by $(T_g/T_w)^{0.55}$.

The resulting formulas related to (2) and (3) respectively, are the following:

$$\alpha_g = \left(1 - \exp\left[-290P_g \left(f \cdot r \cdot \frac{T_w}{T_g}\right)^{0.5} T_w^{-1.5}\right]\right) \left(\frac{T_g}{T_w}\right)^{0.55} \quad (4)$$

$$\alpha_g = 290 \cdot P_g \cdot \left(f \cdot r \cdot \frac{T_w}{T_g}\right)^{0.5} \cdot T_w^{-1.5} \cdot \left(\frac{T_g}{T_w}\right)^{0.55} \quad (5)$$

It has to be borne in mind that α_g can not be higher than one. When this occurs, a default value of one is assumed by the program.

The enclosure that contains the gas has to be constituted by surfaces divided in triangular cells. Some hypotheses are made about them:

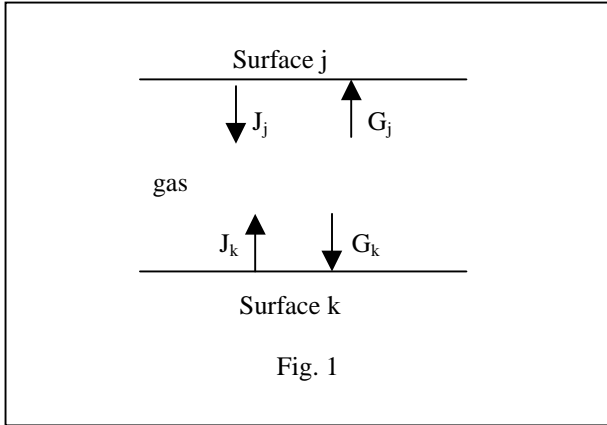
- Each triangular cell is considered to have constant temperature and properties such as emissivity.
- They are diffuse so their emission is no directional and view factors can be used in the study.
- Their emitted, reflected and absorbed radiation do not depend on wavelength (gray surfaces).
- Incident and reflected energy flows are uniform on each surface.
- They are also opaque: there is no energy transmission through them, and according to the Kirchoff law, their emissivity is equal to their absorptivity.

$$\alpha = 1 - \rho \quad (6)$$

$$\varepsilon = \alpha \quad (7)$$

Gas and surface properties (emissivity, pressure, temperature...) are assumed to be one-dimensional and are defined in discrete points along the volume. Gas and cells assumed characteristics at any position within the enclosure result by interpolation of their nearest defined point properties.

Considering the k cell with an area A_k , the net heat flow per surface unit that reaches the surface is calculated in an iterative way, as the difference between the energy radiated by the cell (due to its temperature and reflection) and the incident radiation on it (due to the gas and the rest of cells):



$$\frac{Q_k}{A_k} = J_k - G_k \quad (8)$$

Radiosity (J_k) is composed by cell k emitted radiation because of its temperature and by the portion of incident energy that it reflects.

$$J_k = \varepsilon_k \sigma T_k^4 + \rho_k G_k = \varepsilon_k \sigma T_k^4 + (1 - \varepsilon_k) G_k \quad (9)$$

Irradiation (G_k), the energy that reaches k , can be written as:

$$G_k = \sum_{j=1}^N F_{k \rightarrow j} (\tau_g J_j + \varepsilon_g \sigma T_g^4) \quad (10)$$

As can be seen, G_k is the result of the sum of the energy fraction that leaves each cell j and reaches the cell k plus the emission of the gas volume included between j and k (that is the reason why gas emission is multiplied by the view factor).

The view factor between two cells is defined as:

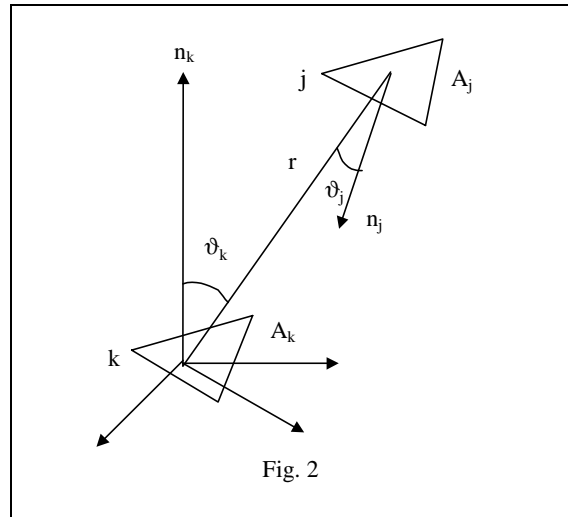
$$F'_{k \rightarrow j} = \frac{\cos \vartheta_k \cos \vartheta_j}{\pi r^2} A_j \quad (11)$$

Where ϑ_k and ϑ_j are the angles that the normal to k and j respectively, forms with the line that joins their barycenters, being r the length of that line. The area and view factor in the above expression should be differential. Thus, results are better when cells are smaller.

However, for reducing errors while conserving the view proportion between each pair of cells, the view factor finally considered will be the result of dividing $F'_{k \rightarrow j}$ by the sum of all corresponding to cell k :

$$F_{k \rightarrow j} = \frac{F'_{k \rightarrow j}}{\sum_{j=1}^N F'_{k \rightarrow j}} \quad (12)$$

By using that view factor, dependency on the cell size can be minimized, being possible to reduce the number of cells that conforms the mesh as well as the computation time.



2 Afterburner radiation study

The first application of this program, which results are presented in this paper, was the thermal analysis of a military turbojet thrust augmentor. However, this study is only focused on radiation. The overall thermal analysis

process is iterative, because wall temperatures are required for radiation heat transfer calculation, being in their turn these temperatures affected by the obtained radiation results. Analysis was performed at Maximum Reheat regime and Sea Level Static condition.

and 7 correspond to those measured by thermocouples placed on them and surface 8 represents the ambient heat dump.

Figures 4 and 5 show contour temperature distribution along the engine external surface and the internal exhaust cone.

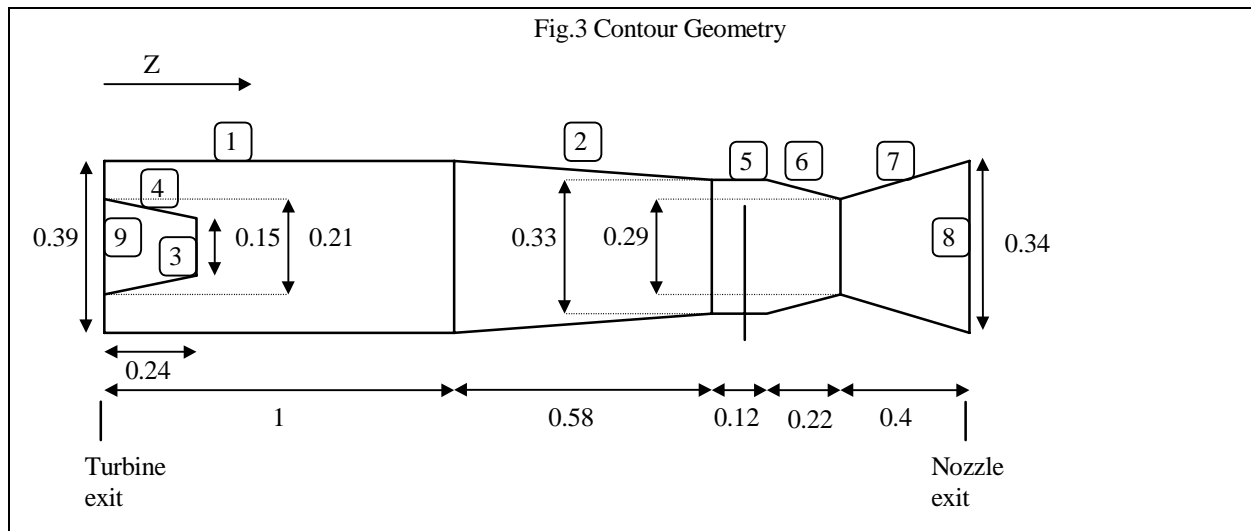


Figure 3 represents the enclosure used in the study. It comprises from the turbine exit until the engine way out, and has been divided in nine surfaces that close the volume completely. Surface numbering and dimensions are shown also in figure 3. Enclosure axis symmetry will allow results to be presented in axial stations.

Surface emissivity varies depending on its state, such as degree of oxidation... In this study, for most of the surfaces, emissivities have been considered of 0.7, which is a typical value for the material and conditions involved in the analysis. Only the nozzle surfaces (6 and 7) have been considered to have an emissivity of 0.8.

2.1 Surface temperature and emissivity

Wall temperatures and emissivities were defined as inputs for radiation calculation.

Surface 1 (post-combustion chamber casing) temperature was supposed to be the same as the temperature of the cooling air that circulates along the liner. Regarding to surfaces 2 and 5, their temperatures were calculated as an average between the liner temperature and the result provided by some experimental correlations. Those correlations try to determine wall temperature when film-cooling efficiency decreases as a result of distance from cooling holes. Finally, temperatures of surfaces 3, 4, 6

Fig. 4. Enclosure external surface temperature (T/T_{ref})

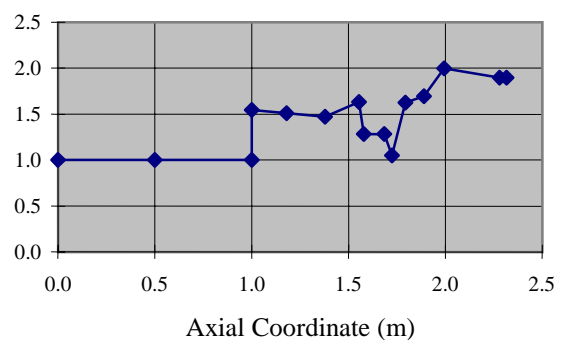


Fig. 5. Temperature along cone surface
(T/Tref)

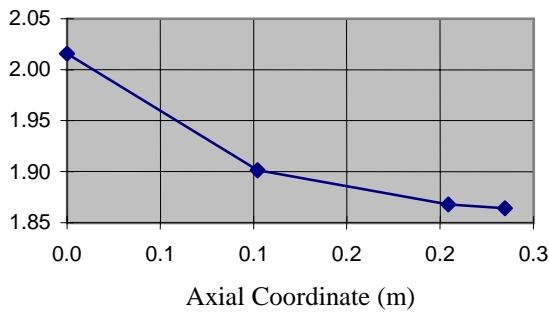
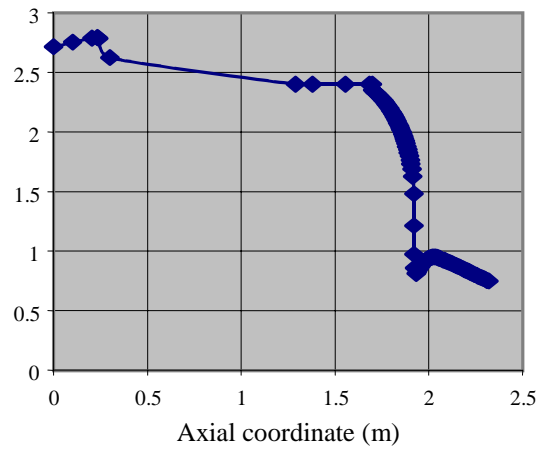


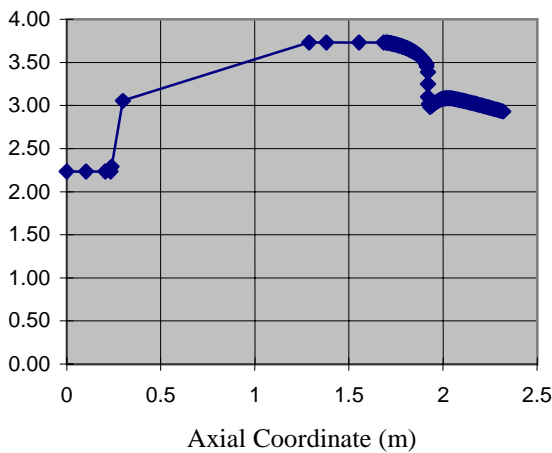
Fig. 7. Gas pressure (P/Pref)



2.2 Gas properties

Gas temperature and pressure distributions along the volume are shown in figures 6 and 7. With them, gas emissivity and absorptivity have been calculated using (2) and (4) respectively. Thus, luminosity effect has been included in the study.

Fig. 6. Gas temperature (T/Tref)



SUP	J (W/m ²)	Q/A (W/m ²)	G _g (W/m ²)	G _N (W/m ²)
1	65860	143456	185164	24152
2	112735	207933	282667	38002
3	115665	91222	193482	13406
4	70012	24479	71654	22836
5	101359	209003	268124	42239
6	74574	200811	231316	44068
7	73093	48657	82839	38911
8	437	139641	80612	59466
9	72862	1392	60216	14038

As can be seen, the highest heat per unit of surface is received by the liner (surfaces 2 & 5). On one hand, the gas is very hot in that zone, and on the other, its emission is not excessively high due to the cold liner temperature considered.

Results in each axial station are presented in figures 8, 9, and 10.

From figure 8 can be observed how the external contour receives the maximum gas irradiation near to the zone where the gas reaches its higher temperature (fig.6). Radiosity distribution is kind of “spiky” (so does the heat), motivated by the differences in wall temperatures promoted by afterburner cooling.

2.3 Results

Global radiosity, net heat per area unit received, gas irradiation and contour irradiation for each surface composing the enclosure, are presented below:

fig. 8. External surface contour results (W/m²)

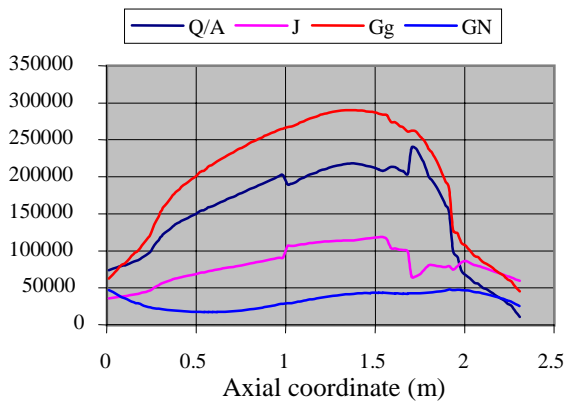
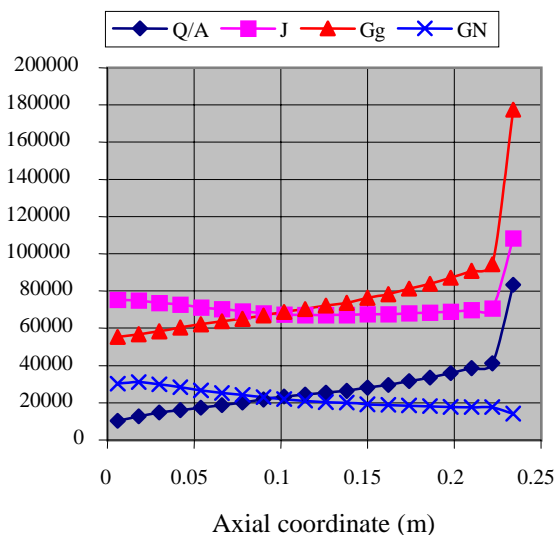


Figure 9 presents the results for the exhaust cone. It can be observed how radiosity and contour irradiation slightly decreases along its surface until the cone lid is reached. Fall in radiosity is mainly motivated by fall in wall temperature (fig.5). Decrease in contour irradiation is the result of the rest of surfaces progressive separation when cone axis coordinate increases (specially the separation of the initial volume lid, which is at very high temperature, and the separation of the cylinder surrounding the cone). Both radiosity and contour irradiation curve tendencies are quite similar, and because their sign is opposite when calculating heat, heat tendency approaches that corresponding to gas irradiation.

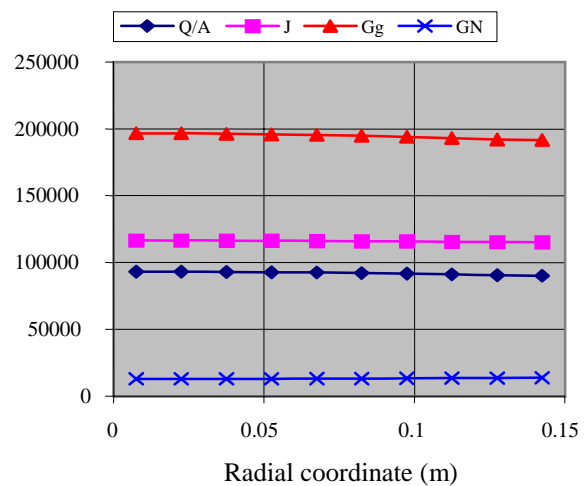
Fig. 9. Cone lateral surface results (W/m²)



By the top of the cone, gas irradiation increases and, although radiosity also raises due to the higher surface temperature and higher incident energy (thus higher reflected radiation), in that zone the final result is the increase in the heat received.

On the cone lid (surface 3) all radiation variables are constant to some degree. However, a slight decrease in the incident heat exists, as the lid edge is being approached from the center (figure 10).

Fig. 10. Cone lid results (W/m²)



2.3.1 Sensitivity analysis

At this point, the influence in radiation of some of the main variables is studied.

- *Cone surface emissivity*

When surface emissivity increases, the emitted energy due to temperature also raises. However, according to Kirchoff law, when emissivity increases so does absorptivity, driving to reflectivity reduction.

As can be seen in figures 11 and 12, the higher cone emissivity the higher net incident heat because of that reduction in reflectivity.

- *Cone lid temperature*

Fig. 11. Cone lateral surface: Q/A variation related to surface emissivity (W/m²)

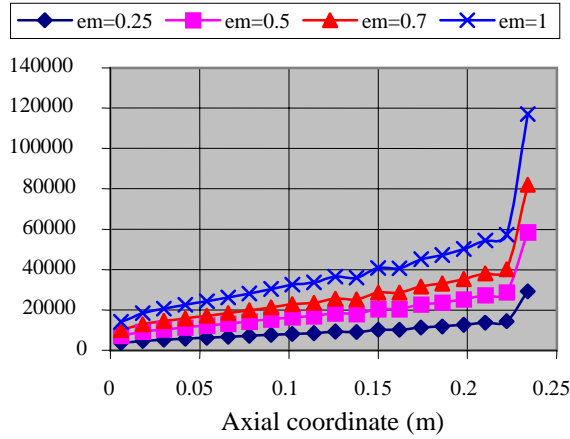


Fig. 12. Cone lid: Q/A variation related to surface emissivity (W/m²)

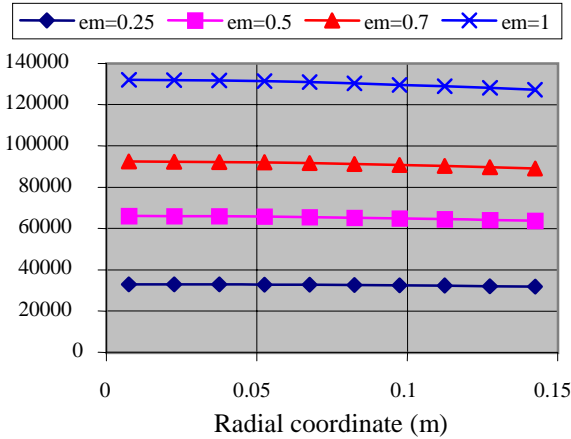
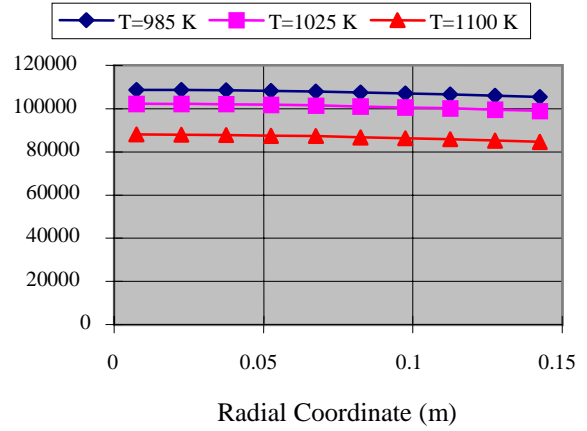


Fig. 13. Cone lid: Q/A variation related to cone lid temperature (W/m²)



important factor for taking into account when evaluating wall received heat.

It has been considered three cases:

1. No variation in gas temperature and pressure. Thus, at the convergent inlet, those magnitudes being the same as at the cone exit station.
2. Lineal increment / decrement in temperature / pressure along the afterburner. From the ones existing at the beginning until the values reached at the nozzle inlet.
3. The presented study case, which is an intermediate situation between the previous ones. Here, gas temperature and pressure have been considered to have a linear evolution along the first part of the afterburner, remaining then constant until the convergent (Fig. 6 and 7).

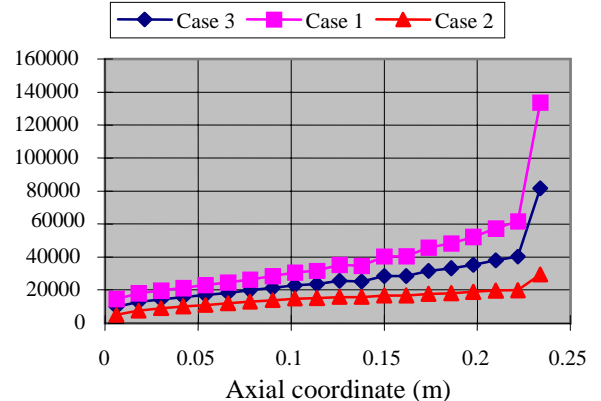
The radiate emission due to a body varies with the fourth power of its temperature. Thus, when reducing cone lid temperature, emission is lower, and as long as incident radiation remains the same, the net heat received by the surface increases (figure 13).

• *Afterburner gas temperature distribution*

Afterburner has been considered the zone included between the cone exit and the nozzle convergent beginning.

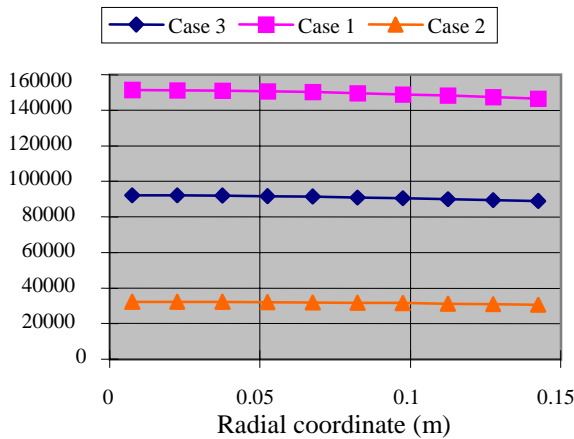
Due to temperature high effect in radiation heat, gas temperature distribution is an

Fig. 14. Cone lateral surface: Q/A variation related to afterburner gas condition (W/m²)



As it was expected, obtained results reflect how the larger space filled with hotter gas, the higher the heat received by the cone.

Fig. 15. Cone lid: Q/A variation related to afterburner gas condition (W/m²)

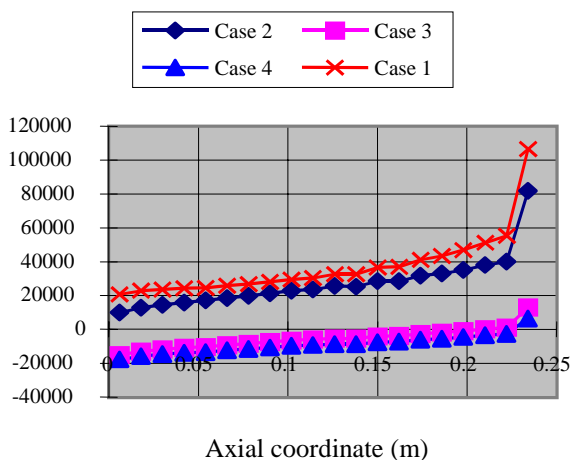


• Gas emissivity

Results obtained when considering different gas emissivities are analyzed.

1. Constant gas emissivity equal to 0.56.
2. Emissivity obtained by using luminosity effect correlation (eq. (2)).

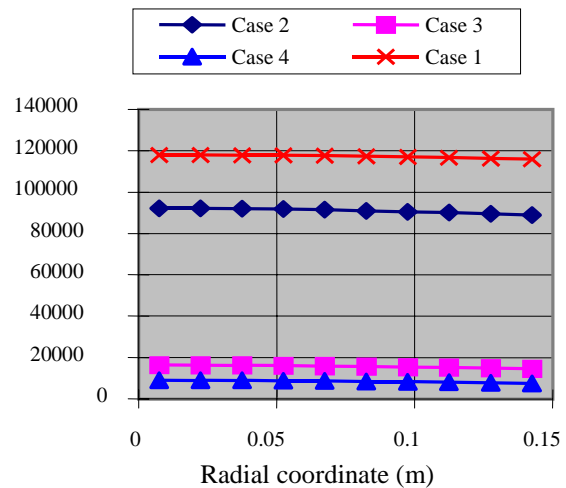
Fig. 16. Cone lateral surface: Q/A variation related to gas emissivity (W/m²)



3. Use of low emissivity correlation (eq. (3)).
4. Use of nonluminosity correlation (obtained by removing L from (2)).

It can be observed how in cases 3 and 4 an interval exists in which the cone surface receives heat instead of emitting. That is due to the low gas irradiation derived from its emissivity decrease.

Fig. 17. Cone lid: Q/A variation related to gas emissivity (W/m²)



Conclusions

Using a simplified definition of the surface view factors, allows a simplified approach to successfully evaluate thermal radiation heat transfer inside engine enclosures. The influence of the main variables can be easily introduced and the computing time is greatly reduced.

This strategy was used to construct a simple computer program which allows a general approximation to carry out thermal analysis of engine components including the effects of thermal radiation.

The results obtained for a military engine afterburner application are summarized in fig 8, 9 & 10. Heat transfer distribution on the walls exposed to the combustion can be seen from them. Logically the higher amount of heat is received by the liner wall.

Sensitivity analyses reflect the influence of different parameters in the results. It is specially surprising the cone lid sensitivity to surface emissivity which varies with oxidation condition.

References

- [1] Lefebvre A. H. *Gas Turbine Combustion*. Hemisphere publishing corporation.
- [2] Holmann J.P. *Heat transfer*. 4th edition, McGraw-Hill, 1976.
- [3] Chapman A. J. *Heat transfer*. 4th edition, Collier Macmillan Publishers, 1984.
- [4] Siegel & Howell. *Thermal radiation heat transfer*. 3rd edition, Taylor & Francis.
- [5] Kreith F., Black W. Z. *La transmision de calor. Principios fundamentales*. Alhambra universidad.
- [6] Ozisik M. Necati. *Heat Transfer. A basic approach*. 1st edition, McGraw-Hill, 1985.